REGULAR ARTICLE

blood advances

Proteogenomic features define subtypes of mantle cell lymphoma

Yuting Yan,[1,2,*] Weihao Chen,[1,2,*] Xinzhou Ge,[3,4,*] Jian Sun,[5,*] Lei Yu,[6,7] Krystine Garcia-Mansfield,[8,9] Xinyi Zhang,[1,2] Ying Yu,[1,2] Wenjie Xiong,[1,2] Dehui Zou,[1,2] Gang An,[1,2] Zhenyu Jia,[6] Patrick Pirrotte,[8,9] Jessica Jingyi Li,[3,4] Zhen Yu,[1,2] Mu Hao,[1,2] Lugui Qiu,[1,2,†] Jianwei Qi,[1,2,†] Lili Wang,[10,11,†] and Shuhua Yi,[1,2,†] for the Chinese Workshop of Indolent Lymphomas

[1]State Key Laboratory of Experimental Hematology, National Clinical Research Center for Blood Diseases, Haihe Laboratory of Cell Ecosystem, Institute of Hematology and Blood Diseases Hospital, Chinese Academy of Medical Sciences and Peking Union Medical College, Tianjin, China; [2]Tianjin Institutes of Health Science, Tianjin, China; [3]Department of Statistics and [4]Department of Computational Medicine, University of California, Los Angeles, CA; [5]Peking Union Medical College Hospital, Chinese Academy of Medical Sciences and Peking Union Medical College, Beijing, China; [6]Department of Botany and Plant Sciences, and [7]Graduate Program in Genetics, Genomics, and Bioinformatics, University of California, Riverside, CA; [8]Cancer and Cell Biology Division, Translational Genomics Research Institute, Phoenix, AZ; [9]Integrated Mass Spectrometry Shared Resource, City of Hope Comprehensive Cancer Center, Duarte, CA; [10]Department of Systems Biology, Beckman Research Institute, City of Hope National Comprehensive Cancer Center, Monrovia, CA; and [11]Division of Hematology/Oncology, Columbia University Medical Center, New York, NY

Key Points

- We present a comprehensive proteogenomic analysis of MCL, integrating proteomics with matched whole-exome and RNA sequencing data.
- We identified 4 molecular subtypes with distinct features, which demonstrate superior prognostic value compared with genomics alone.

Mantle cell lymphoma (MCL) is a biologically heterogeneous B-cell malignancy. Although genomics and transcriptomics have delineated parts of the MCL disease spectrum, proteomics remains largely unexplored. Here, we conducted a comprehensive proteogenomic analysis integrating genomics, transcriptomics, and proteomics on peripheral blood samples from 27 patients with MCL and 4 healthy donors to investigate the translational and posttranslational dimensions of MCL. Our study identified 1296 downregulated and 468 upregulated proteins in MCL cells. The splicing pathways were significantly upregulated at both the mRNA and protein levels, suggesting a critical role for aberrant RNA splicing in MCL pathogenesis. Integration of proteomic data with genetic aberrations revealed immunoglobulin heavy chain variable mutational status and *CCND1* mutation are associated with distinctive transcriptomic and proteomic profiles, which correspond to significant differences in clinical outcomes. A multiomics molecular stratification model incorporating proteomic data showed superior predictive power for patient survival compared with single-omics models (concordance index, 0.83 vs 0.74). This study provides, to our knowledge, the first comprehensive proteogenomic profile of MCL, offering novel insights into its molecular mechanisms and clinical behavior. The identification of molecular subtypes and prognostic protein signatures underscores the potential of proteomics to guide precision medicine strategies for MCL.

Introduction

The molecular landscape of mantle cell lymphoma (MCL) has been extensively characterized by whole-exome sequencing (WES) and transcriptome analysis, uncovering numerous recurrent genetic

Submitted 9 October 2025; accepted 14 February 2026; prepublished online on *Blood Advances* First Edition 5 March 2026. https://doi.org/10.1182/bloodadvances.2025018701.

*Y. Yan, W.C., X.G., and J.S. contributed equally to this study.

†L.Q., J.Q., L.W., and S.Y. contributed equally to this study.

The whole-exome sequencing and RNA sequencing data for the 27 patients with mantle cell lymphoma have been deposited in the Genome Sequence Archive database (BioProject ID PRJCA028747).

The mass spectrometry proteomics data generated in this study have been deposited to the ProteomeXchange Consortium via the Integrated Proteome Resources (iProX) partner repository (the dataset identifier PXD066628).

The full-text version of this article contains a data supplement.

alterations and gene expression changes that contribute to the biological heterogeneity of MCL.[1-6] However, genomic and transcriptomic data alone do not fully capture the complex proteomic landscape that ultimately determines cellular behavior. Proteins, as the functional effectors of cellular processes, have traditionally been studied indirectly through mRNA measurements. Recent advances in mass spectrometry (MS)–based proteomics have allowed direct investigation of the posttranscriptional landscape across various tumors.[7-12] Such approaches have enabled the discovery of distinct molecular subtypes, the elucidation of oncogenic mechanisms, and the identification of therapeutic vulnerabilities. In MCL, most protein-level studies to date have been limited to targeted immunoblotting of selected proteins, lacking a global view of the proteome. A comprehensive and unbiased survey of proteomics in MCL is thus urgently needed.

To address this knowledge gap, we conducted a proteogenomic analysis in primary MCL samples and explored the relationships among genetics, transcriptomics, and proteomics of MCL. Building on our previous study, in which we characterized the genomic landscape of 134 patients with MCL and identified 4 robust genetic subtypes,[5] this study focuses on a representative subset of 27 patients from that cohort for whom sufficient biospecimens were available for deep proteomic profiling.

Methods

Human samples

Normal samples were obtained from the peripheral blood (PB) of 4 healthy donors, whereas tumor samples were collected from the PB of 27 patients with newly diagnosed MCL with PB involvement. All patients and healthy donors were men. All MCL cases harbored the characteristic t(11;14)(q13;q32) translocation with cyclin D1 overexpression and were diagnosed according to World Health Organization criteria. Mononuclear cells from the PB were isolated by density gradient centrifugation using Ficoll-Paque medium (GE Healthcare). Normal B cells and MCL tumor cells were enriched using CD19 magnetic beads followed by flow cytometry–based sorting before protein extraction.

Proteomic analysis

Proteomic profiling was performed using data-independent acquisition MS (DIA-MS). Proteins were extracted, reduced, alkylated, acetone-precipitated, and digested with trypsin following standard protocols. Peptides were desalted, lyophilized, and analyzed on an EASY-nLC 1200 ultrahigh pressure liquid chromatography system (Thermo Fisher Scientific) coupled to an Orbitrap Q Exactive mass spectrometer (Thermo Fisher Scientific), operating in DIA mode. Protein identification and quantification were performed using Proteome Discoverer 2.2 (Thermo Fisher Scientific) and Spectronaut 9.0 (Biognosys) with a false discovery rate (FDR) of 1%. Label-free quantification was conducted using the MaxLFQ algorithm. More protein extraction processes are presented in the supplemental Methods.

Integrative data analysis

Proteomic data preprocessing and missing value imputation were performed using the R package "DEP." Weighted gene coexpression network analysis ("WGCNA" package) was applied to both proteomic and transcriptomic data, with the soft-thresholding power selected based on mean connectivity. Gene Ontology and gene set enrichment analysis were conducted using the R package "clusterProfiler," with a q value < 0.05 considered significant.

Differential expression analyses for RNA sequencing (RNA-seq) and proteomic data were performed using 2-sample *t* tests following trimmed mean of M-values and counts-per-million normalization, respectively. *P* values were adjusted using the Benjamini-Hochberg method. To identify proteins associated with specific genetic variants, patients were first grouped according to the presence or absence of the variant, followed by differential protein expression analysis between the 2 groups under a target FDR of 5%.

We performed the similarity network fusion (SNF) method to integrate data from different omics layers for clustering and visualization,[13] using the "ExecuteSNF.CC" package. The detailed clustering method is described in the supplemental Methods.

Statistical considerations

Survival curves were plotted using the Kaplan-Meier method, and the log-rank test was applied to evaluate the statistical significance of progression-free survival (PFS) and overall survival (OS) between different clusters. Multivariate Cox regression analysis was used to evaluate the independent prognostic value of the MCL International Prognostic Index (MIPI) risk system and individual protein signatures for clinical outcomes of MCL.

Ethics statement

The entire protocols were approved by the human subjects protection committee of the Institute of Hematology and Blood Disease Hospital, the Chinese Academy of Medical Sciences, and the Peking Union Medical College ethics committees (KT2020025-EC-2). All studies were performed after obtaining written informed consent from the patients and in accordance with the Declaration of Helsinki.

Results

To explore the relationship between genotype and phenotype in MCL, we performed protein abundance measurements using MS in DIA mode and integrated these data with corresponding WES and RNA-seq data from matched samples (Figure 1A). The genomic and transcriptomic data for these 27 patients were obtained from our previously published study.[5] The MCL cohort included 27 patients with a broad range of clinical characteristics (Table 1). All patients had bone marrow involvement at diagnosis. The median age was 57 years (range, 44-79), and the 3-year OS in this cohort was 37.5% (95% confidence interval, 22.5%-62.5%), consistent with the inclusion of several high-risk cases.

Integrated proteogenomic and transcriptomic analysis identified key pathways associated with MCL biology

Across all samples, 5702 proteins were consistently detected. Differential analysis between MCL and normal B cells revealed extensive alterations (Figure 1B), with 468 proteins significantly upregulated and 1296 downregulated in MCL (FDR <0.05). The hallmark oncoprotein CCND1 was among the most upregulated proteins. In addition, several novel or unexpected proteins related to cell metabolism and oxidative stress were overexpressed in

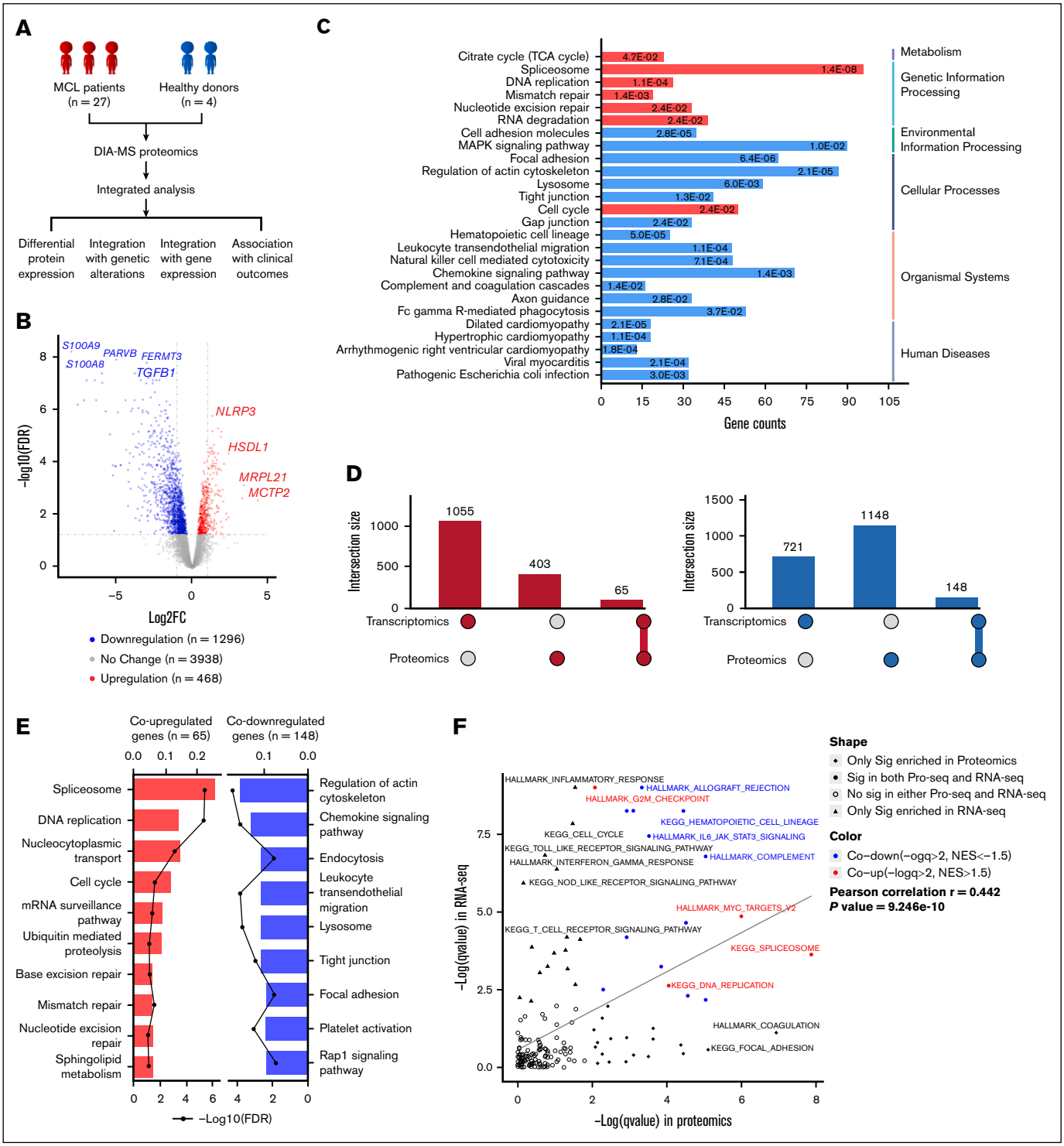

Figure 1. Differential analysis of MCL and normal B cells at the proteomic and transcriptomic levels. (A) Workflow of integrative analysis based on proteogenomics and clinical outcomes. (B) Volcano plot displaying differentially expressed proteins in MCL compared with normal B cells (n = 5702). (C) Functional enrichment analysis of differentially expressed proteins in MCL compared with normal B cells. (D) UpSet plot illustrating the overlap of differentially expressed genes between transcriptomics and proteomics. (E) Pathway enrichment analysis of coupregulated and codownregulated genes at both transcript and protein levels. (F) Gene set enrichment analysis on differentially expressed genes from proteomics and transcriptomics, calculated enrichment *P* values for each pathway, and a scatterplot showing the Pearson correlation of enrichment *P* values for the 2 omics. The red pathways represent the signaling pathways that are significantly upregulated at both multiomics levels in MCL cells, whereas the blue pathways represent the signaling pathways that are significantly downregulated at both multiomics levels in MCL cells. NES, normalized enrichment score.

Table 1. Baseline characteristics of patients

Characteristics	Patients with MCL (N = 27)
Age, median (range), y	57 (44-79)
Male, n (%)	27 (100)
Lactate dehydrogenase >ULN	18 (66.7)
ECOG-PS score of >1	6 (22.2)
WBCs at diagnosis, median (range), $\times 10^9$/L	82.0 (11.8-836.0)
Hemoglobin at diagnosis, median (range), g/dL	11.5 (5.0-14.9)
Platelets at diagnosis, median (range), $\times 10^9$/L	101 (40-362)
Malignant cells fraction in BM detected by FCM, median (range)	73.2 (38.5-95.1)
Clinical group, n (%)	
nnMCL	6 (22)
cMCL	21 (78)
Pathology, n (%)	
Blastic	2 (8)
Classic	23 (92)
Not tested	2
IGHV status, n (%)	
Mutated	7 (26)
Unmutated	20 (74)
MIPI score, n (%)	
Low risk	0 (0)
Intermediate risk	7 (26)
High risk	20 (74)

BM, bone marrow; cMCL, conventional MCL; ECOG-PS, Eastern Cooperative Oncology Group performance status; FCM, flow cytometry; nnMCL, indolent leukemic nonnodal MCL; ULN, upper limit of normal; WBC, white blood cell.

MCL, such as NLRP3, HSDL1, and MRPL21. Conversely, adhesion and cytoskeletal regulators such as PARVB and FERMT3 were markedly downregulated. Functional enrichment analysis of the differentially expressed proteins showed distinct biological themes (Figure 1C). Upregulated proteins were enriched in DNA replication/repair, cell cycle, RNA splicing and processing, and metabolism. This indicates that MCL cells have an enhanced capacity for genome maintenance, transcription/translation processes, and metabolic activity. Contrarily, downregulated proteins were involved in cellular structure, adhesion, immune response, cell-cell interaction, and MAPK signaling. The loss or reduction of these pathways suggests that MCL cells may have defects in immune surveillance and cell adhesion, potentially facilitating immune evasion and dissemination in the body.

We integrated matched RNA-seq and proteomic data to assess how closely mRNA changes mirror protein changes. For each biological pathway, we compared the enrichment trends at the mRNA and protein levels. A comparison of pathway activity changes between transcriptome and proteome showed a mixed pattern (Pearson correlation $r = 0.449$; $P < .01$; supplemental Figure 1). Although some pathways were concordantly upregulated or downregulated at both mRNA and protein levels, many pathways exhibited discordant changes. For instance, the SWItch/Sucrose non-fermentable (SWI/SNF) chromatin-remodeling complex was significantly upregulated at the protein but not mRNA level, whereas pathways such as gap junction assembly were enriched at the transcript level but not at the protein level, suggesting posttranscriptional regulation in these pathways (supplemental Figure 1). We identified 65 consistently upregulated and 148 consistently downregulated genes at both mRNA and protein levels in MCL (Figure 1D). Coupregulated genes were primarily enriched in splicing and DNA replication pathways, whereas codownregulated genes were linked to actin cytoskeleton regulation and chemokine signaling (Figure 1E). Notably, the spliceosome pathway showed strong and consistent upregulation at both RNA and protein levels (Figure 1F; supplemental Figure 2). Detailed examination of the spliceosome components revealed that most core spliceosomal proteins and associated splicing factors (eg, SF3A2, SF3B4, SNRPB, U2AF1, and DDX39B) were uniformly elevated in MCL cells (supplemental Figure 3), indicating that aberrant RNA splicing is a pervasive feature of MCL biology.

Proteogenomic associations with genetic lesions in MCL

We investigated the impact of recurrent genetic aberrations on the MCL proteome. Seventeen lesions were considered: 10 regions of copy number variation (CNV) and 7 frequently mutated genes, based on previous genomic studies.[2,3,5,6] Comparing protein expression between samples with and without each genetic lesion revealed distinct proteomic signatures for key lesions (Figure 2A-B).

Immunoglobulin heavy chain variable (IGHV)–mutated status exerted the strongest influence on the proteome, with numerous proteins differentially expressed between IGHV-mutated and IGHV-unmutated MCL. Compared with unmutated samples, IGHV-mutated samples showed upregulation of DNA damage response (ATM) and mitochondrial proteins (GLS2, PCK2, PPM1K; Figure 2C). By contrast, IGHV-unmutated cases displayed upregulation of proteins implicated in cell cycle and DNA repair (CDK2, HMGB3), structural microtubule-associated proteins, and chaperones (STMN1, SERPINH1, HSPA1B; Figure 2C). Further pathway enrichment analysis showed that IGHV-mutated tumors were enriched in metabolism (oxidative phosphorylation [OXPHOS]; tricarboxylic acid cycle; alanine, aspartate, and glutamate metabolism; and adipogenesis). They also showed enrichment in B-cell receptor (BCR) signaling and antigen processing/presentation pathways, indicating that IGHV-mutated cells maintain B-cell functional programs and interactions with the immune system. Additionally, ribosomal proteins were enriched, suggesting robust protein synthesis in IGHV-mutated MCL. For IGHV-unmutated cells, significant enrichments were observed in proteasome, cell cycle, DNA damage regulation, spliceosome, glutathione metabolism, and interferon response (Figure 2D). These enrichments suggest that IGHV-unmutated cells exhibit a proliferative and stress-adapted phenotype.

CCND1 mutation also affected the proteome. Although *CCND1* translocation occurs in essentially all classic MCL, somatic coding mutations of *CCND1* occur in a subset of cases and have been linked to a more indolent course in some studies.[5] Mutations in *CCND1* were associated with Fcγ receptor–mediated phagocytosis and BCR signaling pathways (Figure 2E). This suggests that subsets of MCL defined by IGHV or *CCND1* status have unique proteomic and signaling profiles that could influence their behavior and therapy response.

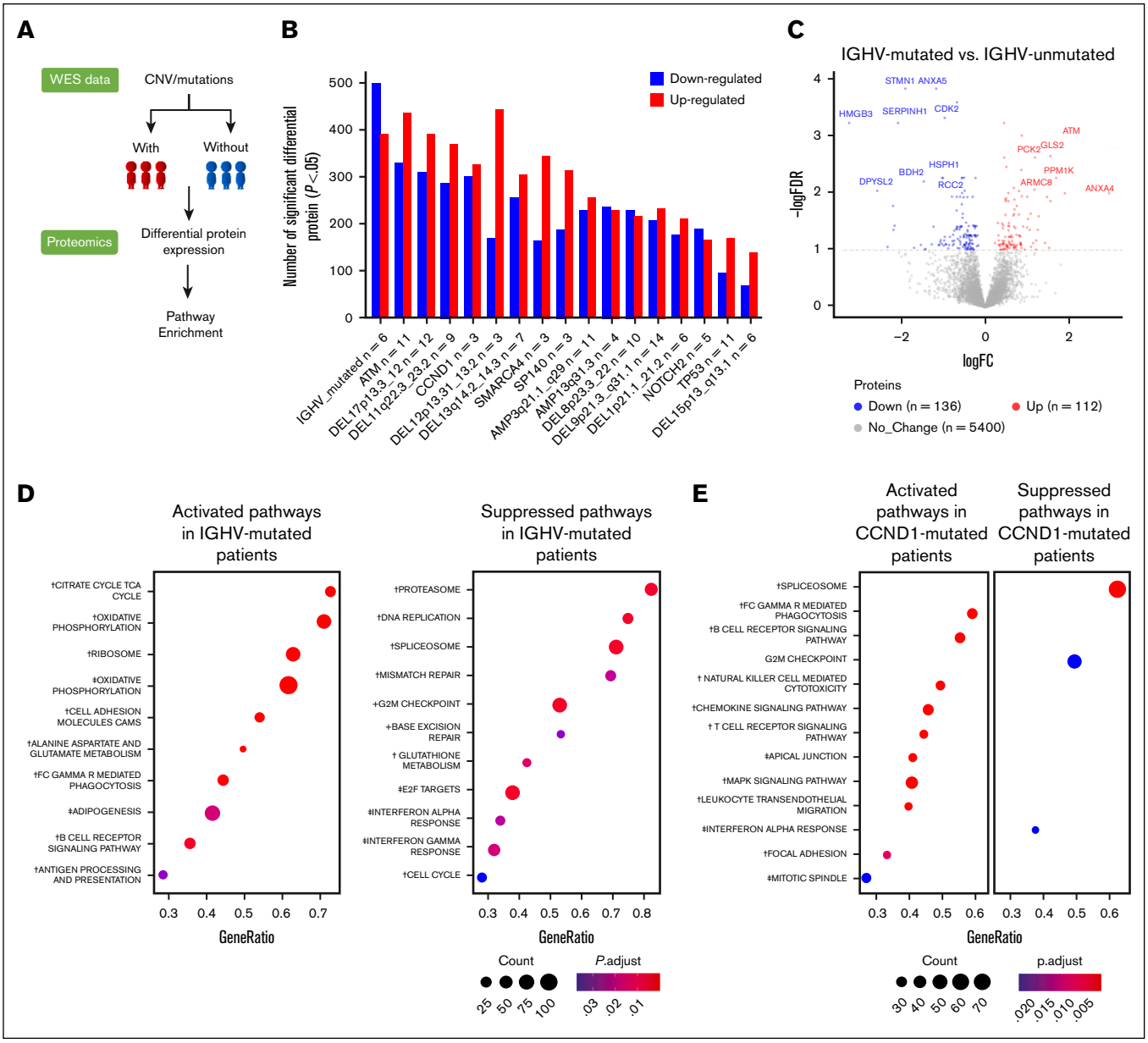

Figure 2. The impact of genetic aberrations on differential protein expression and its enrichment pathways in MCL. (A) Workflow diagram. (B) Number of differentially expressed proteins associated with key genetic aberrations ($P < 0.05$). (C) Volcano plot illustrating significantly upregulated and downregulated proteins in patients with IGHV-mutated MCL vs IGHV-unmutated MCL. (D) Enriched pathways of differential protein expression in patients with IGHV mutation. (E) Enriched pathways of differential protein expression in patients with *CCND1* mutations. Fc, fold change.

To further investigate whether recurrent CNVs exert cis-regulatory effects on protein expression, a total of 297 CNV-protein pairs were analyzed, comprising proteins encoded by genes located within the respective CNV regions. We observed significant associations ($P < 0.05$) for 126 pairs (42.4%), with 117 pairs (39.4%) remaining significant after FDR correction (FDR <0.1); 247 pairs (83.2%) exhibited the expected direction. This concordance rate was highly significant by the binomial test (supplemental Figure 4; $P < 0.001$). However, some genetic events occurred at a very low frequency, each observed in only 3 patients. Therefore, associations involving these alterations should be interpreted with caution and will require validation in larger cohorts.

mRNA-protein concordance in MCL and its biological implications

To explore the relationship between mRNA abundance and protein abundance, we selected overlapping genes from 2 data sets, yielding 5222 mRNA-protein pairs, and calculated the Pearson correlation coefficient across the 27 MCL samples (Figure 3A). Overall, mRNA and protein levels showed a moderate correlation

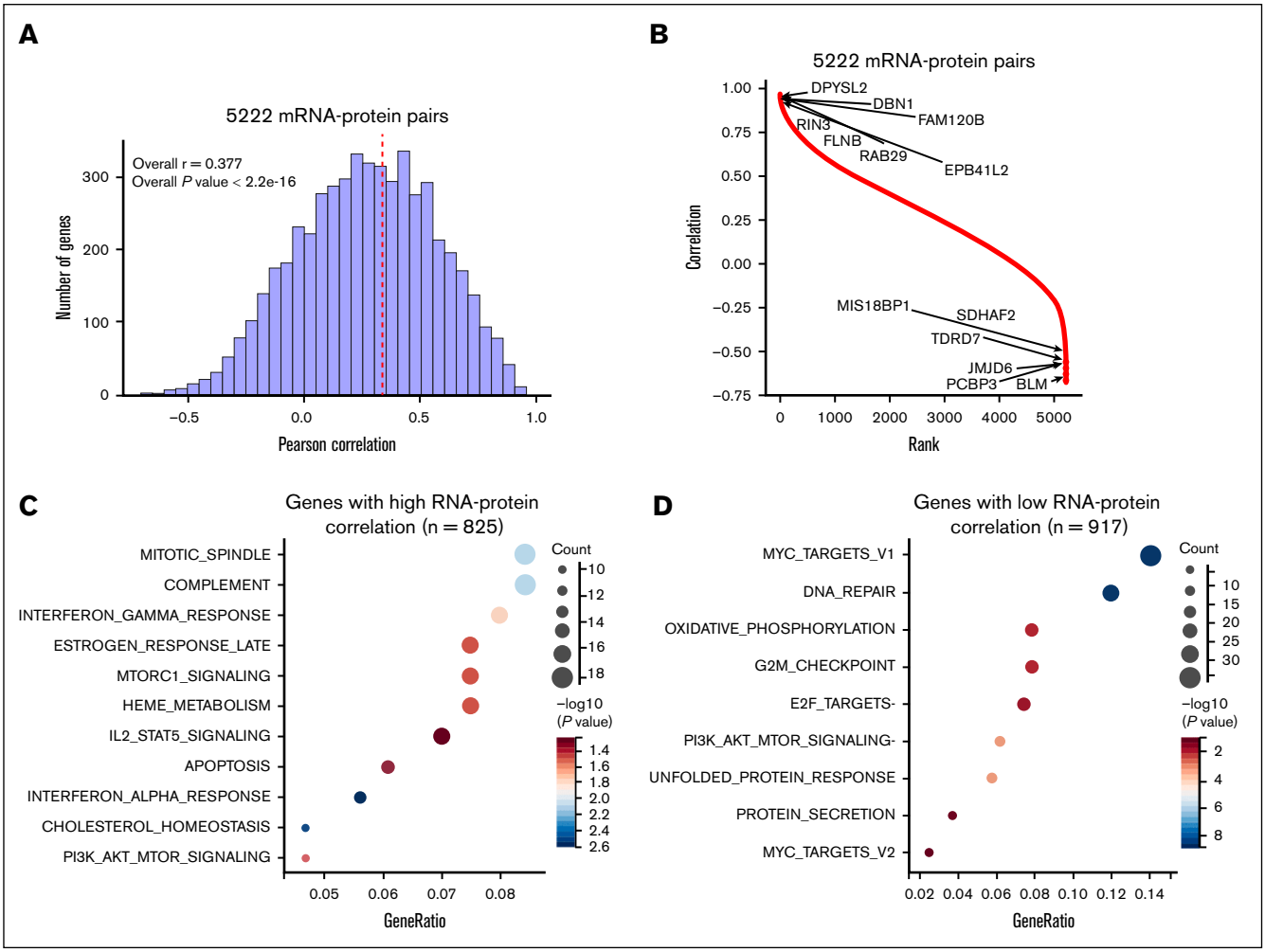

Figure 3. Protein-mRNA concordance and its impact on outcomes in MCL. (A) Pearson correlation distribution between protein and RNA expression across 5222 genes. (B) Ranked correlation coefficients for each protein. (C) Enrichment analysis of high-correlation genes ($r > 0.6$). (D) Enrichment analysis of low-correlation genes ($r < 0.3$).

($r = 0.377$), indicating that although transcriptional control is operative, posttranscriptional regulation is also widespread.

By ranking genes according to mRNA-protein correlation coefficients (Figure 3B), we identified sets of genes at the extremes that offer insight into MCL biology. Genes with the highest positive correlations, including *DPYSL2*, *DBN1*, *RIN3*, *FAM120B*, *FLNB*, and *EPB41L2*, were mainly involved in cytoskeletal organization, cell migration, membrane trafficking, and signaling. The tight mRNA-protein coupling suggests that in MCL cells, these cytoskeletal/migratory proteins are regulated mostly at the transcriptional level. In contrast, genes with the strongest negative correlations, including *MIS18BP1*, *SDHAF2*, *TDRD7*, *JMJD6*, *PCBP3*, and *BLM*, were related to DNA replication, chromatin regulation, and posttranscriptional regulation. The discordance between mRNA and protein levels suggests robust posttranscriptional control. For example, their mRNAs may be present, but translation is inhibited or proteins are rapidly degraded. We categorized genes according to their mRNA-protein correlation, defining high concordance as $r > 0.6$ (n = 825) and low concordance as $r < 0.3$ (n = 927). In total, genes with high mRNA-protein correlations were enriched in pathways related to the mitotic spindle, immune response regulation, and signal transduction (Figure 3C). These are processes in which a concerted gene expression program may require the simultaneous production of many proteins, making transcriptional coregulation effective. In contrast, most genes with low concordance were enriched in hallmark oncogenic pathways, such as MYC targets, DNA repair, and cell cycle (Figure 3D). This indicates that critical regulators of proliferation and genome integrity are subject to complex regulation beyond transcription in MCL. For instance, MYC-driven genes may be modulated by microRNAs or ubiquitin-mediated degradation, and many cell cycle or DNA repair proteins could be controlled by activation/inactivation rather than abundance.

Additionally, we observed that the degree of mRNA-protein correlation varied with MCL subtypes. Samples with blastoid/pleomorphic morphology had significantly higher overall mRNA-protein correlations than classic MCL, and IGHV-unmutated cases exhibited higher concordance than IGHV-mutated cases (supplemental Figure 5). These findings imply that more aggressive MCL operates with a more streamlined and efficient expression program, potentially meeting the demands of rapid proliferation. In comparison, indolent MCLs may tolerate more

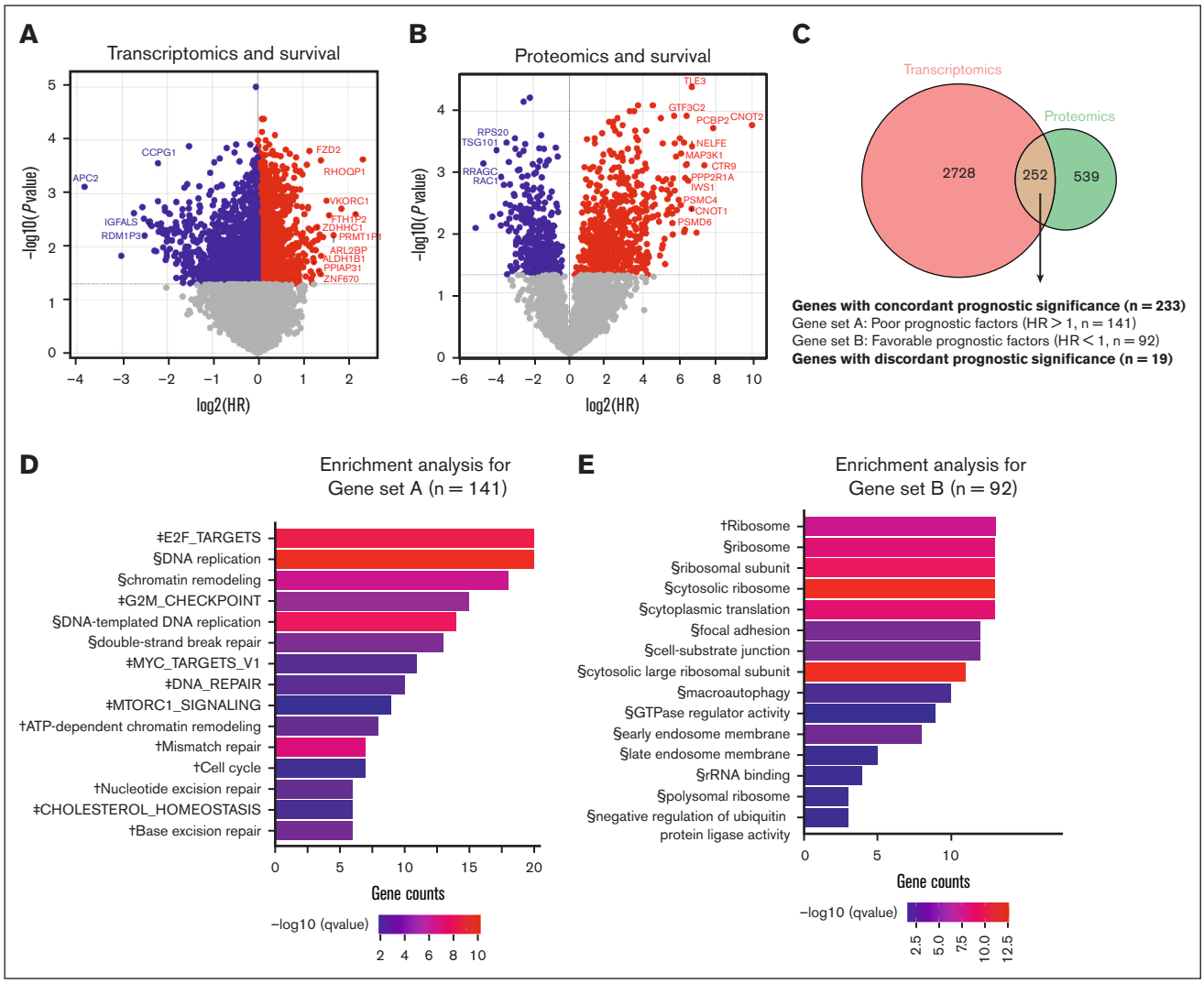

Figure 4. Gene set associated with MCL survival prognosis. (A) Volcano plot of prognostic mRNAs from univariate Cox analysis ($P < 0.05$), showing 1821 mRNAs associated with longer survival (hazard ratio [HR] < 1; blue) and 1678 mRNAs associated with shorter survival (HR > 1; red). (B) Volcano plot of prognostic proteins from univariate Cox analysis ($P < 0.05$), showing 347 proteins associated with longer survival (HR < 1; blue) and 602 proteins associated with shorter survival (HR > 1; red). (C) Venn diagram showing overlap between transcriptomic and proteomic data in the identification of shared prognostic genes. A total of 252 shared prognostic genes were identified, of which 233 showed concordant prognostic significance, including 141 poor prognostic factors (Gene set A; $P < 0.05$; HR >1) and 92 favorable prognostic factors (Gene set B; $P < 0.05$; HR <1). The remaining 19 genes showed opposite prognostic significance between the transcript and protein levels. (D) Enrichment analysis of Gene set A (poor prognostic factors). (E) Enrichment analysis of Gene set B (favorable prognostic factors).

discordance, possibly reflecting the greater influence of regulatory checkpoints.

Prognostic signatures at the transcript and protein levels

We next sought to identify genes and proteins with prognostic significance in our cohort and determine how the integration of multiomics data could refine risk stratification in MCL. Despite the limited sample size, multiple candidate prognostic biomarkers were identified. At the mRNA level, we found 2980 RNAs associated with prognosis. Among them, APC2 and CCPG1, which are related to cell cycle and proliferation, were significantly associated with poor outcomes. FZD2 and RHOQP1, which are related to cell proliferation, differentiation, and motility, were significantly associated with better survival (Figure 4A). We note that these correlations do not imply causation, but can point to important biological differences. At the protein level, we identified 791 proteins associated with prognosis, of which 493 were linked to inferior survival and 298 to favorable survival. Specifically, CNOT1/2, PCBP2, and CTR9, which are associated with post-transcriptional regulation and oncogene expression, showed significant correlations with inferior survival, whereas higher protein levels of RRAGC, TSG101, and RPS20, which are associated with tumor development, showed significant correlations with favorable survival (Figure 4B).

Intersecting transcript- and protein-level prognostic markers identified 252 shared genes, of which 233 showed concordant

prognostic significance, whereas 19 showed discordant prognostic associations between the transcript and protein levels (Figure 4C). This convergence provides higher confidence that these genes play a role in MCL progression. Among the 233 concordant genes, 141 were poor prognostic factors (hazard ratio [HR] >1; Gene set A), and 92 were favorable prognostic factors (HR <1; Gene set B; Figure 4D). Pathway enrichment analysis revealed that Gene set A was enriched in cell proliferation and DNA replication pathways (Figure 4E). Gene set B was enriched in ribosome, protein synthesis, and focal adhesion pathways, reflecting a more differentiated or stable cellular state that curbs aggressive behavior (Figure 4E).

Integrative multiomics clustering reveals 4 molecular subgroups

To explore the molecular heterogeneity of MCL, we first performed consensus clustering separately on proteomic and transcriptomic data. Using the partitioning around medoids algorithm with 500 bootstrap iterations, both omics layers stratified patients into 3 subgroups (supplemental Figure 6). However, suboptimal silhouette coefficients and limited concordance in cross-comparisons between the 2 single-omics classifications indicated insufficient stratification robustness (supplemental Table 1). These results suggest that single-omics approaches have limited power to robustly stratify patients with MCL. Therefore, to integrate the multilayered molecular data and classify patients with MCL into molecularly distinct subgroups, we subsequently developed a multiomics integration model.

Through Cox regression analysis, we included key genetic lesions, including 7 recurrent mutations and 10 CNVs, along with the top 300 survival-associated transcripts and the top 300 survival-associated proteins as input features for SNF clustering. Detailed survival statistics for the transcriptomic and proteomic features included in the model are listed in supplemental Table 2. We identified 4 clusters, designated C1 to C4, each defined by key driver genetic alterations, RNAs, and proteins (Figure 5A). The average silhouette width for clustering was 0.78, indicating a robust separation among clusters (supplemental Figure 7A-B). Specifically, C1 was characterized by IGHV-mutated status, *CCND1* mutation, and absence of *del9p* or *del11q*; C2 correlated with *NSD2* mutation and higher MIPI scores; and C3 and C4 were more strongly associated with *TP53* abnormalities and *del9p*, with *del1p21* particularly frequent in C3 (Figure 5A; supplemental Figure 7C). These findings were similar to those of our previous WES-based study, in which 4 genomic subgroups were also identified.[5] In this study, patients in the C1 group remained unchanged between single WES level and multiomics level, reinforcing the robustness of this indolent subgroup. However, cases grouped in C2 to C4 by genomics alone were further distinguished into separate clusters upon multiomics integration (Figure 5B). Four multiomics clusters exhibited significantly different prognosis (OS, C1-C4: not reached, 35.1, 19.0, and 12.5 months, respectively, $P < 0.001$; PFS, C1-C4: not reached, 22.7, 14.2, and 5.4 months, respectively, $P < 0.001$; Figure 5C). The multiomics model for assessing prognosis achieved a concordance index (C-index) of 0.83 for OS, which was higher than the C-index of 0.74 in the single-omics model. Using the cluster assignment as an ordinal risk score, the multiomics clustering demonstrated superior discriminative ability for both OS (area under the curve: 0.846 vs 0.796) and PFS (area under the curve: 0.843 vs 0.764) compared with single-omics clustering (supplemental Figure 8). Within this cohort, the multiomics classification provided somewhat improved prognostic discrimination compared with the single-omics clustering. These findings are exploratory and require validation in larger independent series. Moreover, the protein signature remained independently prognostic after adjustment for MIPI risk. This suggests that these molecular subtypes capture risk that is not fully explained by clinical indices, highlighting a potential role for proteomic biomarkers in risk stratification.

To gain biological insight into each subgroup, cluster-specific gene set enrichment analysis was performed (supplemental Figures 9 and 10). C1 demonstrated extensive enrichment of BCR signaling pathways, consistent with antigen-experienced, ongoing BCR activity in these IGHV-mutated tumors. It also had high enrichment of OXPHOS, mitochondrial metabolism, ribosome, and mRNA translation pathways, indicating a metabolically active yet controlled proliferation. Immune-regulatory pathways were more active in C1, suggesting these tumors might have better interaction with immune cells. In C2, we observed moderate downregulation of cellular metabolic pathways unlike C1. However, RNA splicing, DNA replication, and immune-related pathways were slightly upregulated compared with C1. This cluster seems to occupy an intermediate biological state, not as metabolically active as C1, but without the severe suppression of BCR signaling and immune pathways seen in C3/C4. C3 was characterized by marked downregulation of BCR signaling, immune response, and apoptosis pathways. Meanwhile, C3 showed upregulation of OXPHOS, cell adhesion, and extracellular matrix interactions, which might indicate a tendency for these cells to reside in protective niches. C4 exhibited the most extreme profile, with significant downregulation of ribosome, BCR signaling, and immune-mediated pathways, coupled with notable upregulation of DNA replication/repair, p53, and cell cycle pathways.

We calculated RNA-protein correlation coefficients for each subgroup. We observed significantly discrepant correlations between RNA and protein expression across the subgroups. Interestingly, we noted a trend of increasing mRNA-protein correlation from C1 to C4 (supplemental Figure 11). This finding is consistent with our earlier observation (supplemental Figure 5) that aggressive MCL exhibits tighter transcriptional-translational coupling. In aggressive tumors, measuring either mRNA or protein might similarly capture the activity of critical pathways, whereas in indolent tumors, protein levels might provide additional information beyond mRNA due to greater posttranscriptional regulation.

Given the complexity and inapplicability of the entire multiomics grouping in practice, we developed a simplified multiomics model. We performed differential expression analysis using the limma package to identify the top 5 differentially expressed features in each cluster. From these results, we selected 6 DNA alterations, 7 RNA transcripts, and 3 protein signatures that were biologically or clinically relevant to disease progression and tumor development. These features were then used to construct a simplified molecular classification model (Figure 5D). This parsimonious model successfully recapitulated the risk stratification of the full multiomics analysis, achieving 100% concordance across the 27-patient

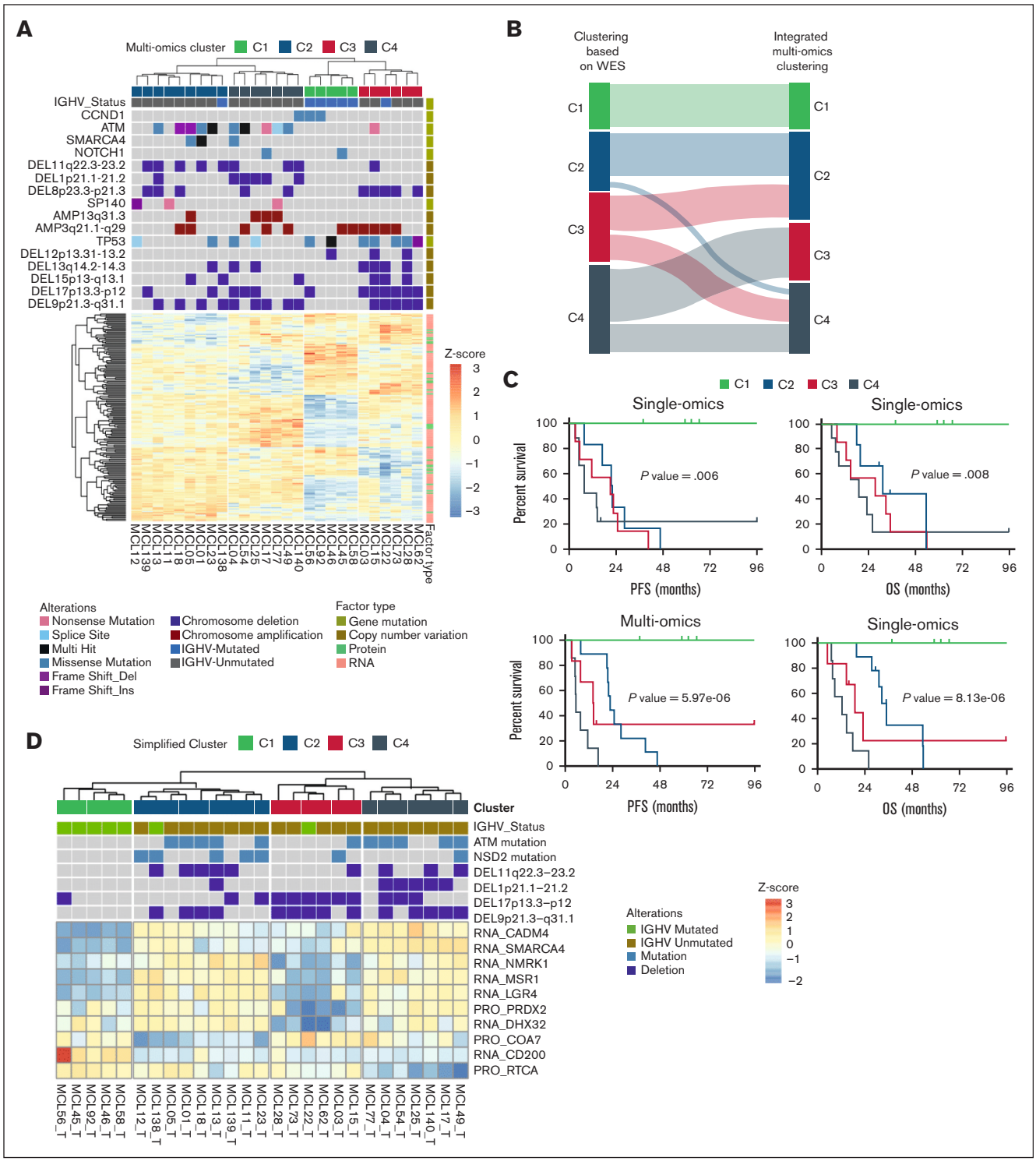

Figure 5. The identification of 4 molecular subgroups based on integrated multiomics clustering and clinical implications in MCL. (A) Unsupervised clustering of multiomics profiles reveals patient clusters. The heat map visualizes the top discriminant RNA and protein signatures associated with each subgroup. Color scale represents z score normalized expression values. (B) Sankey diagram showing redistribution of clusters between the clustering based on single-omics and the clustering based on multiomics. The width of each band is proportional to the number of patients. (C) PFS and OS between 4 subgroups based on single-omics clustering (PFS, $P = 0.006$; OS, $P = 0.008$) and multiomics clustering (PFS, $P < 0.001$; OS, $P < 0.001$). (D) Simplified multiomics clustering incorporating representative 7 genetics, 7 RNA, and 3 protein signatures. Del, deletion; Ins, insertion.

cohort. Although requiring independent validation, this simplified approach highlights the translational potential of our findings and could evolve into a practical tool to guide MCL management and optimize therapeutic selection.

Discussion

MCL is an uncommon subtype of B-cell lymphoma, accounting for 4% to 9% of non-Hodgkin lymphoma in high-income countries.[14] Multiple groundbreaking studies have already profiled the genomic, transcriptomic, and epigenetic landscapes of MCL,[1-6,15,16] shedding light on its molecular heterogeneity, pathogenesis, and mechanisms of drug resistance. However, to our knowledge, no comprehensive proteomic profiling of MCL had been reported to date. Hence, we addressed that gap by integrating proteomics with genomics and transcriptomics in primary MCL samples. Our analysis yielded, to our knowledge, the first proteogenomic atlas of MCL, uncovering potential biology and defining molecular subgroups with relatively distinct features and outcomes.

Our proteomic profiling of MCL cells revealed widespread pathway dysregulation. Proteins involved in metabolism, spliceosome, and DNA replication/repair were upregulated, underscoring enhanced genetic information processing. These alterations implicate that aberrant posttranscriptional regulation and genomic instability as central to MCL pathogenesis and its high proliferative activity. Conversely, pathways related to cellular structure and immune function were broadly downregulated, including MAPK signaling, cytoskeletal organization, cell adhesion, and immune effector responses. *FERMT3* downregulation might impair stromal adhesion and immune recognition, thereby promoting tumor cell migration and resistance to cytotoxic killing. Similarly, reduced S100A8/9 in tumor cells might reflect an immunosuppressive niche, as these proteins are known to modulate inflammation. These findings point to impaired immune surveillance, weakened cytotoxic function, and diminished intercellular junctions, which may together facilitate immune evasion and systemic dissemination in MCL.

The spliceosome, a crucial component in the generation of mature mRNA and an important posttranscriptional regulatory mechanism,[17-19] was significantly upregulated at both RNA and protein levels in MCL. Clinical and mechanistic studies have confirmed that mutations affecting the spliceosome or splicing factors are recurrent genetic abnormalities in various cancers. For example, the *SF3B1* mutation is commonly observed in myeloid malignancies and chronic lymphocytic leukemia.[20-22] Such spliceosome alterations disrupt key cellular signaling pathways, including those involved in DNA damage response and B-cell signaling, driving tumorigenesis and drug resistance.[17,23,24] A large-scale genomic study reported novel mutations in RNA-binding proteins in MCL, including *HNRNPH1*, which regulates alternative pre-mRNA splicing and is associated with poor prognosis.[6] Elevated expression levels of heterogeneous nuclear ribonucleoproteins were also observed. In our study, we found significant upregulation of genes or proteins associated with spliceosome components, such as *DDX39B*, *SNRPB*, *U2AF1*, *SF3B4*, and *SF3A2*, supporting spliceosome dysregulation as a common pathogenic feature in MCL. Additionally, our differential protein expression analysis showed that the spliceosome pathway was downregulated in patients with IGHV-mutated status and *CCND1* mutations. In previous research, we identified that patients with MCL harboring these 2 mutations represent a distinctive subset with favorable outcomes. Thus, the upregulation of the spliceosome pathway may represent the high-risk biology of MCL. Investigating whether targeting spliceosome abnormalities could provide therapeutic benefits in specific MCL subgroups warrants further exploration. Although we identified spliceosome dysregulation as a hallmark of MCL, this study did not comprehensively characterize specific alternative splicing isoforms or structural variants. Further investigations into these splicing aberrations and their mechanistic contributions to MCL pathogenesis are currently underway.

Functional protein abundance cannot be reliably inferred from transcriptional data alone, due to extensive posttranscriptional regulation.[25-28] In our cohort, the correlation between RNA and protein in MCL was also limited (a median correlation coefficient of 0.377). This value is similar to previous studies that reported comparable RNA-protein correlation levels in other cancers, such as 0.18 in chronic lymphocytic leukemia, 0.31 in acute myeloid leukemia, 0.39 in breast cancer, and 0.47 in colorectal cancer.[9-11,26] Gene expression is shaped by multilayered controls encompassing mRNA transcription, processing, transport, translation, modification, and degradation.[25,28] Dysregulation at any stage of these processes may mediate or affect the occurrence of various diseases, such as cancer.[29-31] These findings reveal a dual regulatory mechanism in tumors: although tight transcription-translation coupling supports the proliferative and metabolic demands of tumor cells, extensive posttranscriptional regulation simultaneously drives dysregulated cell cycle progression and impairs DNA repair. Consequently, relying solely on mRNA measurements may misrepresent the functional state of these pathways.

Notably, aggressive MCL subtypes exhibited higher mRNA-protein correlation (supplemental Figures 5 and 11). We hypothesize that highly proliferative tumors maintain tight transcriptional-translational coupling to meet the metabolic and structural demands of rapid growth, minimizing posttranscriptional buffering as an adaptive strategy. This heightened coupling may render aggressive cells particularly vulnerable to proteotoxic stress, providing a mechanistic rationale for the efficacy of proteasome inhibitors in this context. Conversely, the lower concordance in indolent cases likely reflects a more quiescent state with greater posttranscriptional buffering or protein turnover. These insights underscore the power of multiomics integration to delineate aggressive MCL phenotypes beyond genomics alone.

In our previous publication, we have described different subgroups of MCL based on genomic data.[5] The integration of multiple omics layers (DNA, RNA, and protein data) into a unified classification model resulted in a higher C-index, indicating better prognostic accuracy for patients with MCL. This is quite promising for a 27-patient discovery data set. If validated, this refined stratification will provide a more nuanced molecular landscape with therapeutic implications. For the C1 group, there was no change between single-omics and multiomics. This group, featured by mutated IGHV and *CCND1* and hyperactive BCR signaling and OXPHOS pathways, suggests potential sensitivity to Bruton tyrosine kinase or OXPHOS inhibitors. C2 was enriched with *NSD2* mutations. Jain et al reported that *NSD2* mutations may be associated with blast transformation and resistance to ibrutinib alone.[32] In contrast, the

C3 and C4 groups, characterized by *TP53* abnormalities and *del9p*, had the worst clinical outcome. This result is consistent with previous studies.[33-35] C3 and C4 were mainly downregulated in immune-related pathways, implying that these clusters may be associated with immune-evasive phenotypes. But C4 had a greater emphasis on unchecked cell cycle progression and replicative stress, whereas C3 showed a shift toward metabolic adaptation and adhesion. High proliferative activity and immune escape may jointly contribute to the extremely poor prognosis of C4. It also raises the possibility that immune-based therapies, such as bispecific antibodies or chimeric antigen receptor T-cell therapy, might be less effective unless combined with strategies to reverse that immune-cold state. In contrast, the strong cell cycle and DNA repair signals in cluster C4 suggest vulnerability to cell cycle kinase inhibitors (eg, CDK4/6 inhibitors) or DNA damage exacerbation (eg, ataxia telangiectasia and Rad3-related [ATR] inhibitors). Collectively, this multiomics landscape refines risk stratification and provides a basis for future precision medicine approaches in MCL.

We acknowledge several limitations in our study. First, our clustering was derived from a relatively small cohort of 27 patients with MCL and lacked independent validation due to the rarity of the disease and the difficulty in obtaining high-purity samples. Furthermore, our cohort was exclusively constituted of male patients with PB involvement. Although this design allowed for a focused analysis of tumor cell–intrinsic proteomic differences, it implies that caution should be exercised when extrapolating our findings to pure nodal disease or female patients. Finally, despite the high sensitivity of DIA-MS, the technique is subject to methodological constraints. Due to differences in protein abundance and potential masking effects, it is not possible to detect every expressed protein within the cellular proteome.

Nonetheless, our study presents a comprehensive proteogenomic characterization of MCL. By integrating multiomics data, we identified 4 molecular subtypes and demonstrated that proteomic information substantially improves risk stratification. Biologically, we highlighted the prominence of the spliceosome and other posttranscriptional modulators in MCL, suggesting new avenues for therapeutic intervention. This work establishes the unique biological and clinical value of protein abundance data in MCL. Additionally, we provide a comprehensive protein expression reference map to support future research and translational efforts.

Acknowledgments

This work was supported by grants from the National Nature Science Foundation of China (82570248, 82170193, 82370197, 82200215), the Chinese Academy of Medical Sciences Innovation Fund for Medical Sciences (2025-I2M-C&T-B-073), Beijing Xisike Clinical Oncology Research Foundation (Y-2024AZ(BTK)ZD–0074), and the Shenzhen Science and Technology Innovation Commission (JCYJ20240813140803005).

Authorship

Contribution: S.Y. and L.W. conceptualized the study design; Y. Yan collected samples, performed experiments, and created the figures; W.C. and Y. Yan wrote the manuscript; Y. Yan, X.G., J.S., L.Y., K.G.-M., Z.J., P.P., and J.J.L. conducted data analysis and provided statistical support; X.Z., Y. Yu., W.X., D.Z., G.A., Z.Y., and M.H. acquired the data and managed the patients; and L.W., L.Q., J.Q., and S.Y. critically revised the manuscript and approved the final version.

Conflict-of-interest disclosure: The authors declare no competing financial interests.

A complete list of the members of the Chinese Workshop of Indolent Lymphomas appears in "Appendix."

ORCID profiles: Y. Yan, 0000-0002-9355-2984; J.S., 0000-0003-4997-2604; Y. Yu, 0000-0001-7362-2925; D.Z., 0000-0002-8135-4913; G.A., 0000-0003-4922-4614; Z.J., 0000-0002-1428-904X; P.P., 0000-0003-1360-6039; J.J.L., 0000-0002-9288-5648; M.H., 0000-0001-8621-4840; L.Q., 0000-0002-7438-8277; S.Y., 0000-0002-6291-812X.

Correspondence: Shuhua Yi, Institute of Hematology and Blood Disease Hospital, Chinese Academy of Medical Sciences and Peking, 288 Nanjing Rd, Tianjin 30020, China; email: yishuhua@ihcams.ac.cn; Lili Wang, Division of Hematology & Oncology, Columbia University Medical Center, 630 W 168th St, New York, NY 10032; email: lw3282@cumc.columbia.edu; Jianwei Qi, Institute of Hematology and Blood Disease Hospital, Chinese Academy of Medical Sciences and Peking, 288 Nanjing Rd, Tianjin 30020, China; email: qijianwei@ihcams.ac.cn; and Lugui Qiu, Institute of Hematology and Blood Disease Hospital, Chinese Academy of Medical Sciences and Peking, 288 Nanjing Rd, Tianjin 30020, China; email: qiulg@ihcams.ac.cn.

Appendix

The members of the Chinese Workshop of Indolent Lymphomas are Yuting Yan, Weihao Chen, Xinyi Zhang, Ying Yu, Wenjie Xiong, Dehui Zou, Gang An, Zhen Yu, Mu Hao, Lugui Qiu, and Shuhua Yi.

References

1. Kridel R, Meissner B, Rogic S, et al. Whole transcriptome sequencing reveals recurrent NOTCH1 mutations in mantle cell lymphoma. *Blood*. 2012;119(9):1963-1971.
2. Beà S, Valdés-Mas R, Navarro A, et al. Landscape of somatic mutations and clonal evolution in mantle cell lymphoma. *Proc Natl Acad Sci U S A*. 2013;110(45):18250-18255.
3. Zhang J, Jima D, Moffitt AB, et al. The genomic landscape of mantle cell lymphoma is related to the epigenetically determined chromatin state of normal B cells. *Blood*. 2014;123(19):2988-2996.
4. Nadeu F, Martin-Garcia D, Clot G, et al. Genomic and epigenomic insights into the origin, pathogenesis, and clinical behavior of mantle cell lymphoma subtypes. *Blood*. 2020;136(12):1419-1432.

5. Yi S, Yan Y, Jin M, et al. Genomic and transcriptomic profiling reveals distinct molecular subsets associated with outcomes in mantle cell lymphoma. *J Clin Invest*. 2022;132(3):e153283.
6. Pararajalingam P, Coyle KM, Arthur SE, et al. Coding and noncoding drivers of mantle cell lymphoma identified through exome and genome sequencing. *Blood*. 2020;136(5):572-584.
7. Johansson HJ, Socciarelli F, Vacanti NM, et al; Consortia Oslo Breast Cancer Research Consortium OSBREAC. Breast cancer quantitative proteome and proteogenomic landscape. *Nat Commun*. 2019;10(1):1600.
8. Zhang H, Liu T, Zhang Z, et al; CPTAC Investigators. Integrated proteogenomic characterization of human high-grade serous ovarian cancer. *Cell*. 2016;166(3):755-765.
9. Mertins P, Mani DR, Ruggles KV, et al; NCI CPTAC. Proteogenomics connects somatic mutations to signalling in breast cancer. *Nature*. 2016; 534(7605):55-62.
10. Meier-Abt F, Lu J, Cannizzaro E, et al. The protein landscape of chronic lymphocytic leukemia. *Blood*. 2021;138(24):2514-2525.
11. Kramer MH, Zhang Q, Sprung R, et al. Proteomic and phosphoproteomic landscapes of acute myeloid leukemia. *Blood*. 2022;140(13):1533-1548.
12. Akbani R, Ng PK, Werner HM, et al. A pan-cancer proteomic perspective on The Cancer Genome Atlas. *Nat Commun*. 2014;5:3887.
13. Wang B, Mezlini AM, Demir F, et al. Similarity network fusion for aggregating data types on a genomic scale. *Nat Methods*. 2014;11(3):333-337.
14. Vose JM. Mantle cell lymphoma: 2017 update on diagnosis, risk-stratification, and clinical management. *Am J Hematol*. 2017;92(8):806-813.
15. Agarwal R, Chan YC, Tam CS, et al. Dynamic molecular monitoring reveals that SWI-SNF mutations mediate resistance to ibrutinib plus venetoclax in mantle cell lymphoma. *Nat Med*. 2019;25(1):119-129.
16. Zhang L, Yao Y, Zhang S, et al. Metabolic reprogramming toward oxidative phosphorylation identifies a therapeutic target for mantle cell lymphoma. *Sci Transl Med*. 2019;11(491):eaau1167.
17. Wang E, Aifantis I. RNA splicing and cancer. *Trends Cancer*. 2020;6(8):631-644.
18. Obeng EA, Stewart C, Abdel-Wahab O. Altered RNA processing in cancer pathogenesis and therapy. *Cancer Discov*. 2019;9(11):1493-1510.
19. Yang H, Beutler B, Zhang D. Emerging roles of spliceosome in cancer and immunity. *Protein Cell*. 2022;13(8):559-579.
20. Palomo L, Meggendorfer M, Hutter S, et al. Molecular landscape and clonal architecture of adult myelodysplastic/myeloproliferative neoplasms. *Blood*. 2020;136(16):1851-1862.
21. Quesada V, Conde L, Villamor N, et al. Exome sequencing identifies recurrent mutations of the splicing factor SF3B1 gene in chronic lymphocytic leukemia. *Nat Genet*. 2011;44(1):47-52.
22. Li Z, He Z, Wang J, Kong G. RNA splicing factors in normal hematopoiesis and hematologic malignancies: novel therapeutic targets and strategies. *J Leukoc Biol*. 2023;113(2):149-163.
23. Wang L, Brooks AN, Fan J, et al. Transcriptomic characterization of SF3B1 mutation reveals its pleiotropic effects in chronic lymphocytic leukemia. *Cancer cell*. 2016;30(5):750-763.
24. Ten Hacken E, Valentin R, Regis FFD, et al. Splicing modulation sensitizes chronic lymphocytic leukemia cells to venetoclax by remodeling mitochondrial apoptotic dependencies. *JCI insight*. 2018;3(19):e121438.
25. Vogel C, Marcotte EM. Insights into the regulation of protein abundance from proteomic and transcriptomic analyses. *Nat Rev Genet*. 2012;13(4): 227-232.
26. Zhang B, Wang J, Wang X, et al; NCI CPTAC. Proteogenomic characterization of human colon and rectal cancer. *Nature*. 2014;513(7518):382-387.
27. Liu Y, Beyer A, Aebersold R. On the dependency of cellular protein levels on mRNA abundance. *Cell*. 2016;165(3):535-550.
28. Buccitelli C, Selbach M. mRNAs, proteins and the emerging principles of gene expression control. *Nat Rev Genet*. 2020;21(10):630-644.
29. Lin S, Gregory RI. MicroRNA biogenesis pathways in cancer. *Nat Rev Cancer*. 2015;15(6):321-333.
30. Tahmasebi S, Khoutorsky A, Mathews MB, Sonenberg N. Translation deregulation in human disease. *Nat Rev Mol Cell Biol*. 2018;19(12):791-807.
31. Delaunay S, Helm M, Frye M. RNA modifications in physiology and disease: towards clinical applications. *Nat Rev Genet*. 2024;25(2):104-122.
32. Jain P, Kanagal-Shamanna R, Zhang S, et al. Long-term outcomes and mutation profiling of patients with mantle cell lymphoma (MCL) who discontinued ibrutinib. *Br J Haematol*. 2018;183(4):578-587.
33. Clot G, Jares P, Giné E, et al. A gene signature that distinguishes conventional and leukemic nonnodal mantle cell lymphoma helps predict outcome. *Blood*. 2018;132(4):413-422.
34. Ferrero S, Rossi D, Rinaldi A, et al. KMT2D mutations and TP53 disruptions are poor prognostic biomarkers in mantle cell lymphoma receiving high-dose therapy: a FIL study. *Haematologica*. 2020;105(6):1604-1612.
35. Delfau-Larue MH, Klapper W, Berger F, et al; European Mantle Cell Lymphoma Network. High-dose cytarabine does not overcome the adverse prognostic value of CDKN2A and TP53 deletions in mantle cell lymphoma. *Blood*. 2015;126(5):604-611.